

The Effects of Temperature on the Spherical Crystallization of Salicylic Acid*

Y. KAWASHIMA, M. OKUMURA and H. TAKENAKA

Gifu College of Pharmacy, 5-6-1, Mitahora-higashi, Gifu 502 (Japan)

(Received March 23, 1983; in revised form October 15, 1983)

SUMMARY

The effects of temperature on the spherical crystallization of salicylic acid were investigated. An ethanolic solution of salicylic acid held at 40 °C was introduced into a well-dispersed mixture of chloroform and water at 5 to 30 °C. By increasing the temperature, larger agglomerates with less spherical forms composed of larger crystals were obtained. The mass growth rate of the agglomerated crystals was described by the mass transfer-controlled kinetics. The growth rate coefficient at 30 °C was significantly smaller than those at 10 and 20 °C. The linear growth rate of the agglomerated crystals increased with increasing temperature, but did not depend upon the solute bulk concentration.

INTRODUCTION

The present authors [1] have developed a novel crystallization technique which could transform the fine crystals themselves into a spherical dense agglomerate during crystallization in liquid. Due to the spherical form of the resultant crystals, this technique was termed 'spherical crystallization'. In this process, as a crystallization solvent, a mixture of three partially miscible solvents, e.g. ethanol-water-chloroform, was used. When the composition of the mixture was correctly chosen, a small amount of solvent, termed 'bridging liquid', was liberated from the system. This liquid collected the crystals produced during crystallization and transformed them into a spherical form.

Sodium theophylline monohydrate crystals produced by salting out were simultaneously agglomerated in a mixture of an ethylenediamine solution of theophylline, an aqueous solution of sodium chloride, ethanol and chloroform, with a suitable composition [2]. Spherically agglomerated crystals of theophylline were prepared directly during reaction by agitating a mixture of chloroform, ethanol (or methanol) and water containing ethylenediamine and theophylline [3].

In the present study, the needle-like salicylic acid crystals were agglomerated into a spherical form during crystallization with agitation in a mixture of ethanol, water and chloroform. The aim of the study was to elucidate the effects of crystallization temperature on the physicochemical properties of the resultant agglomerated crystals, agglomeration behavior and the spherical crystallization kinetics.

EXPERIMENTAL

Spherical crystallization technique

Fifty ml of ethanol solution containing 12.5 g of salicylic acid held at 40 °C was poured into a mixture of chloroform (9 ml) and water (250 ml) in a cylindrical vessel (500 ml, i.d., 84 mm), which was uniformly agitated with a turbine-type agitator with 6 blades. In the present study, a small amount of chloroform liberated from the mixture acted as a bridging liquid, which preferentially wetted the salicylic acid crystals and agglomerated them into a spherical form. The agitator was centrally located at 1 cm from the bottom as shown in Fig. 1. The vessel was thermally controlled at 5, 10, 20 or 30 °C, in a water bath. After starting the crystallization, 2 ml of aliquot was sampled at a suitable

*Part VI of 'Spherical Crystallization'.

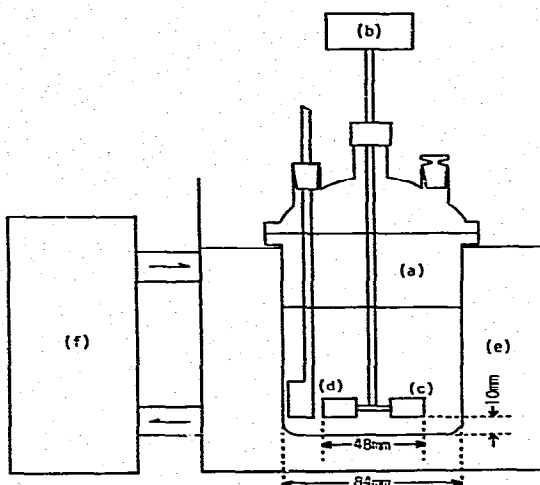


Fig. 1. Apparatus for spherical crystallization of salicylic acid. (a), Cylindrical vessel (500 ml); (b), motor; (c), turbine-type agitator (6 blades, agitation speed 600 rpm); (d), baffle; (e), water bath (temperature 5 to 30 °C); (f), regulator.

interval from the system using a pipette with a cotton plug. The sample was filtered with a membrane filter (pore diameter, 0.45 μm) and was diluted with a mixture of ethanol and water with the same composition of the crystallization solvent used. The concentration of salicylic acid was analyzed spectrophotometrically at 296 nm. At the same time, a small amount of agglomerated crystals in the system was sampled. The agglomerates sampled were dried for 24 h at room temperature and their weights w and numbers n were measured. The total agglomerate numbers in the system N were determined by substituting n , w and the total agglomerate weight W crystallized from the system into eqn. (1).

$$N = \frac{W}{w} n \quad (1)$$

Measurement of the micromeritic properties of the agglomerates

The bulk density of the agglomerates was represented by the loosest packing density in a measuring cylinder (25 ml). The agglomerate size was measured by a sieve analysis or by a photographic counting method using a particle size analyzer (TGZ-3, Carl Zeiss). The apparent density ρ_{ap} of the agglomerate was determined by substituting the average

diameter d , the number n and the weight w of the agglomerates sampled into eqn. (2).

$$\rho_{ap} = \frac{w}{\sum \frac{\pi}{6} d^3 n} \quad (2)$$

The sphericity of the agglomerate was defined by the Wadell [4] sphericity s expressed by eqn. (3).

$$s = \frac{\text{diameter of circle with projected area of particle}}{\text{diameter of minimum circle circumscribed by particle}} \quad (3)$$

The agglomerate was dispersed in a liquid paraffin mounted on a slide glass and the photograph of the constituent crystals of the agglomerate was taken through a microscope. The crystal size was represented by the length of the crystal.

RESULTS AND DISCUSSION

Effect of temperature on the micromeritic properties of the agglomerated crystals

The average diameter of the agglomerated crystals at 1 h residence time determined by a sieve analysis is plotted against the crystallization temperature in Fig. 2. The size variation of the agglomerates is represented by a

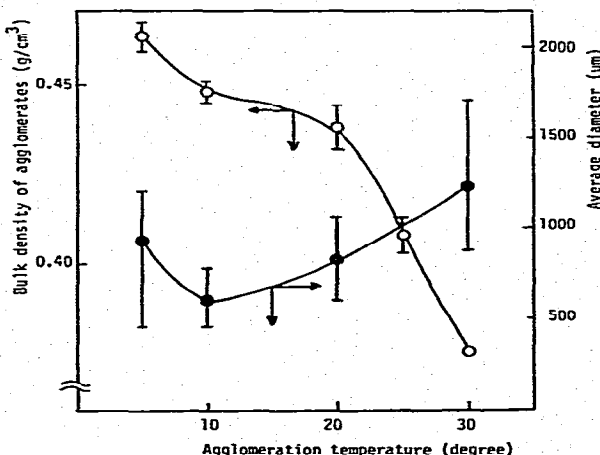


Fig. 2. Effects of temperature on the average diameter and the shape of agglomerates. ●, Average diameter of agglomerates; ○, bulk density of agglomerates.

standard deviation bar. The average size of the agglomerates was the smallest at the crystallization temperature 10 °C. At temperatures higher or lower than 10 °C, the agglomerate size and the size variation increased. In the previous paper [2, 3], it was found that the agglomerate size increased with an increase in the amount of bridging liquid used for agglomeration. The solubility of chloroform in the ethanol-water mixture at various temperatures was investigated, since the agglomerate size in the present study depended on the amount of chloroform liberated from the system. With increasing temperature, the phase separation line moved down a little as shown in Fig. 3. Chloroform was miscible in the region M above the phase separation line, while it was immiscible in the region I below the line. The finding in Fig. 3 indicated that the solubility of chloroform increased a little with increase in temperature. The recovery of salicylic acid from the system and the constituent crystal size of salicylic acid in the agglomerate at various temperatures are tabulated in Table 1. With increasing temperature, the recovery of the crystals in Table 1 decreased drastically compared with the increased solubility of chloroform in Fig. 3. Therefore, at high temperatures, the amount of available chloroform for agglomeration of the crystals apparently increased, resulting a yield of large agglomerates. It was found in previous investigations [5, 6] that fine particles required less amount of bridging liquid

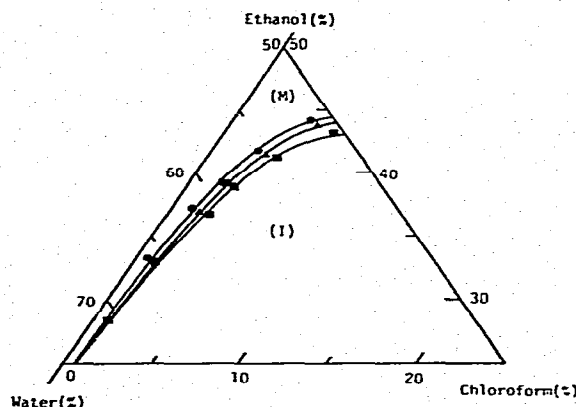


Fig. 3. Effect of temperature on the phase separation curve. Agglomeration temperature: ●, 10 °C; ▲, 20 °C; ■, 30 °C. Chloroform is miscible in region M above the solid line and immiscible in region I below the solid line.

TABLE 1
Effect of temperature on recovery and size distribution of crystals

Crystallization temperature	Recovery of crystals	Size distribution of constituent crystals (μm) (16% - 50% - 84%)
5°	94%	41 - 83 - 121
10°	92%	63 - 106 - 150
20°	88%	85 - 166 - 245
30°	78%	81 - 173 - 270

for agglomeration and produced larger agglomerates than coarse particles, since the adhesive force of fine particles with bridging liquid was stronger than that of coarse particles. At low temperatures (e.g. 5 °C), the recovery of the crystals increased, whereas the constituent crystal size and the solubility of chloroform in the solvent mixture decreased. Therefore, it was assumed that the amount of available chloroform was enough for agglomeration of fine particles, resulting in the large agglomerates produced at 5 °C in Fig. 2.

The bulk density of the agglomerates decreased with increasing crystallization temperature in Fig. 2. This finding suggested that the large agglomerates produced at high temperatures were bulky. The relationship between the sphericity and the average projected area diameter of the agglomerates is exhibited in Fig. 4. It was found that the larger agglomerates were less spherical. Therefore, they were loosely compacted in a container, leading to low bulk density as seen in Fig. 2.

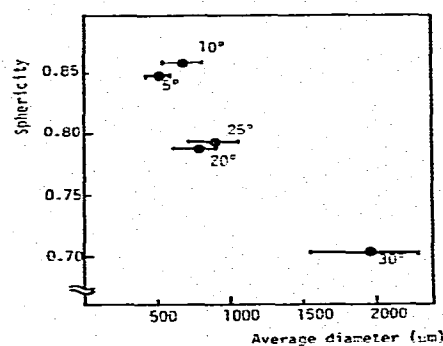


Fig. 4. Relationship between the sphericity and the average particle diameter of agglomerates as a function of temperature.

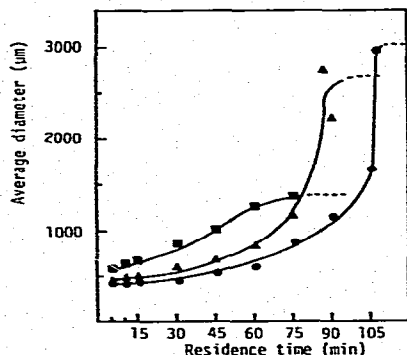
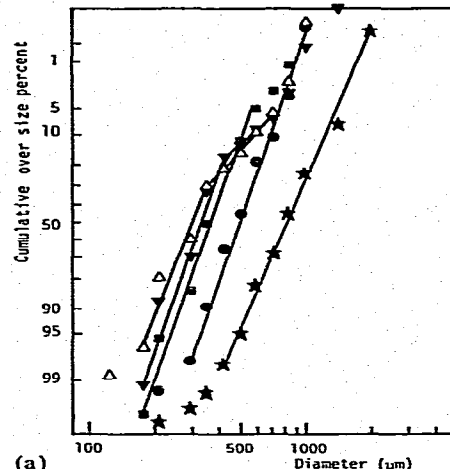


Fig. 5. Average diameter of agglomerates as a function of residence time. Agglomeration temperature: ●, 10 °C; ▲, 20 °C; ■, 30 °C.

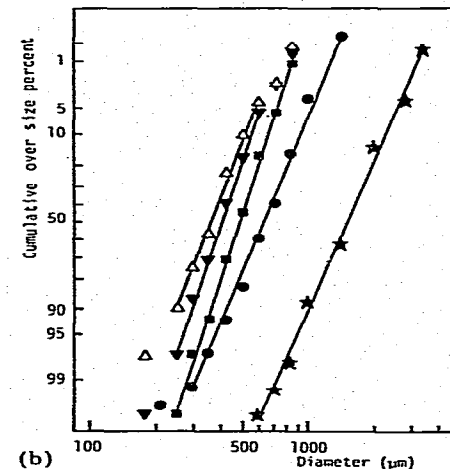
Effect of temperature on agglomeration behavior

The average diameters of the agglomerates determined by sieve analysis are plotted as a function of the residence time at various agglomeration temperatures in Fig. 5. At higher temperatures, the larger agglomerates were produced initially and the equilibrium state attained more rapidly than at lower temperatures. At low temperatures, it was a characteristic that the growth rate of the crystal was slow at the initial stage, but became faster at the later stage. This phenomenon might be interpreted by the fact that at low temperatures the fine crystals were produced as shown in Table 1. It was found in a previous study [7], that the agglomerate of fine particles was compacted during agglomeration more closely than that of coarse particles. The bridging liquid which moved to the outer surface of the agglomerate of fine crystals by capillary suction induced by compaction during agglomeration might promote further agglomeration at the later stage.

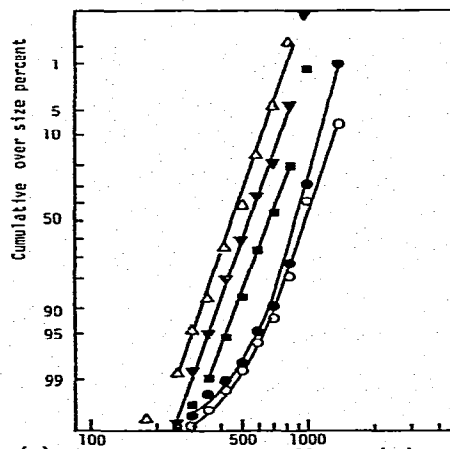
The size distribution of the agglomerated crystals is shown as a function of residence time in Fig. 6. All size distributions obeyed a log-normal form. The slopes of the straight lines on a log-normal probability graph were almost constant irrespective of the residence time and the crystallization temperature. The geometric standard deviation of the agglomerates was around 1.36 for all agglomerates, suggesting that the distribution form of the agglomerates was preserved during spherical crystallization as found in a previous paper [8].



(a)



(b)



(c)

Fig. 6. Size distribution of agglomerates. Agglomeration temperature: (a), 10 °C; (b), 20 °C; (c), 30 °C. Residence time (min): △, 5; ▼, 15; ■, 30; ●, 60; ○, 75; ★, 90.

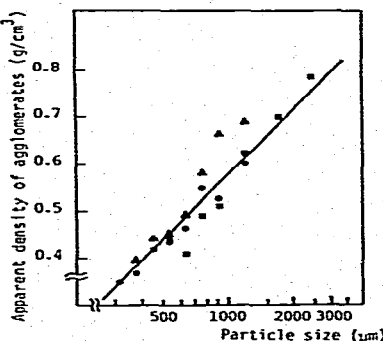


Fig. 7. Relationship between the particle size and the apparent density of agglomerates. Agglomeration temperature: 10 °C. Residence time (min): ●, 30; ▲, 60; ■, 90.

During the agglomeration process, the agglomerated crystals were compacted due to the collisions of agglomerates with each other or with the vessel wall. A linear relationship between the apparent density and the size of the agglomerate was found as shown in Fig. 7. This finding indicated that large agglomerates were compacted more closely than fine ones irrespective of the residence time, since the collision energy of larger agglomerates was greater than that of smaller ones.

Effect of temperature on the spherical crystallization kinetics

The mass growth rate R of crystals from solution can be explained generally by eqn. (4).

$$R = K(C - C_{eq})^n \quad (4)$$

where K is constant, C and C_{eq} are bulk solute concentrations at time t and equilibrium saturation concentration, and n is the overall order of growth. The mass of crystals W is represented by eqn. (5).

$$W = (C_i - C)V \quad (5)$$

where C_i is the initial bulk solute concentration and V is the volume of solution. The mass growth rate eqn. (6) is derived by differentiating eqn. (5) with respect to time t .

$$R = \frac{dW}{dt} = \frac{d}{dt}(C_i - C)V = -\frac{d}{dt}(C - C_{eq})V \quad (6)$$

It was found that the bulk solute concentration reached the equilibrium saturation

concentration 18 min after the start of crystallization. The change in bulk solute concentration at $t < 18$ min was expressed by the first-order kinetic eqn. (7).

$$\ln(C - C_{eq}) = -k_1 t + \ln(C_0 - C_{eq}) \quad (7)$$

where C_0 is the concentration extrapolated to $t = 0$, k_1 is a constant, i.e. 0.309, 0.293 and 0.361 for 10, 20 and 30 °C, respectively, and $\ln(C_0 - C_{eq})$ is 6.92, 7.06 and 7.69 for 10, 20 and 30 °C, respectively. The mass growth rate of the agglomerated crystals in this study was expressed by eqn. (8), which was obtained by inserting eqn. (7) into eqn. (6).

$$R = -V k_1 \exp[-k_1 t + \ln(C_0 - C_{eq})] \quad (8)$$

The mass growth rates are plotted against $(C - C_{eq})$ in Fig. 8, exhibiting the linear correlations. The finding indicated that n in eqn. (4) was equal to 1, suggesting that the kinetics was described by the mass transfer-controlled growth [9]. When the temperature was 30 °C, the growth rate coefficient was significantly smaller than those at 10 and 20 °C.

The mass of crystals W is also expressed by eqn. (9).

$$\begin{aligned} W &= \frac{\pi}{6} l^3 \rho N \\ &= (C_i - C)V \\ &= [C_i - C_{eq} - (C - C_{eq})]V \end{aligned} \quad (9)$$

where l is the average diameter of the spherically agglomerated crystals, N is the total

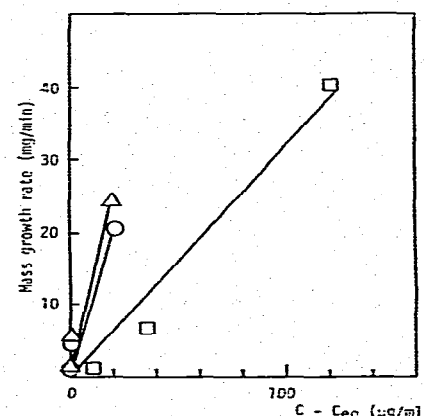


Fig. 8. Effect of temperature on mass growth rate. Agglomeration temperature: ○, 10 °C; ▲, 20 °C; ■, 30 °C.

agglomerated crystal numbers at time t and ρ is the density of the agglomerated crystals. The total number of agglomerated crystals in the system are plotted against the residence time as shown in Fig. 9(a). As expected, the total number of agglomerates decreased rapidly at high crystallization temperature. At the initial stage ($t < 18$), the data exhibited straight lines on a semilogarithmic graph as shown in Fig. 9(b), indicating that the agglomeration process was described by first-order kinetics.

$$\ln N = -k_2 t + \ln N_0 \quad (10)$$

where N and N_0 are the total numbers of agglomerates in the system at residence time t and extrapolated to $t = 0$, respectively, and k_2 is a constant. The constant increased with increasing crystallization temperature, *i.e.* 0.0327, 0.038 and 0.0549 for 10, 20 and 30 °C, respectively. At low temperature, the initial number of crystals produced was greater than at high temperature. N_0 , assumed to be the number of crystal nuclei, increased with decreasing crystallization temperature as shown in Fig. 9(b).

A linear relationship between the crystal nuclei number and the extent of supersaturation was found in Fig. 10. The extent of supersaturation S was defined by eqn. (11).

$$S = \frac{C}{C_{eq}} \quad (11)$$

The finding in Fig. 10 agreed with the previous study by Elworthy and Worthington [10]. They found that the finer crystals were

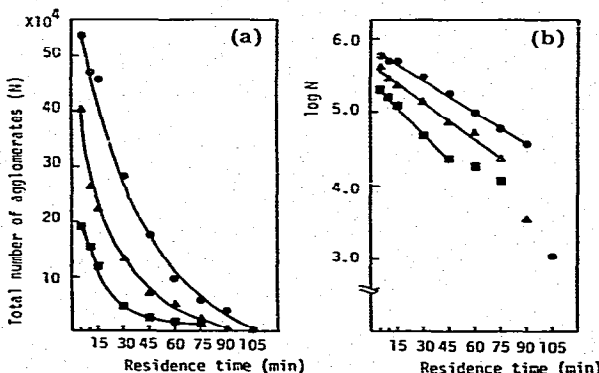


Fig. 9. Number of agglomerates N as a function of residence time. (a), N versus residence time; (b), $\log N$ versus residence time. Agglomeration temperature: ●, 10 °C; ▲, 20 °C; ■, 30 °C.

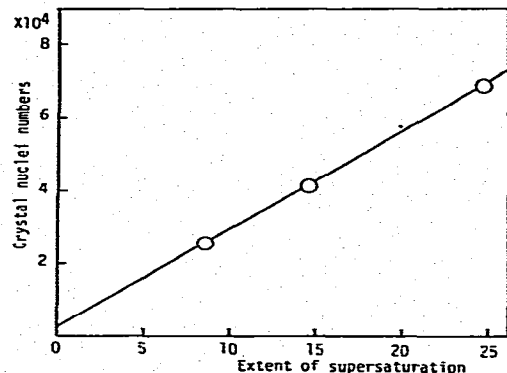


Fig. 10. Relationship between the crystal nuclei numbers and the extent of supersaturation.

obtained at greater supersaturation in the crystallization of sulfadiazine.

The average agglomerated crystal diameter l can be expressed by eqn. (12), derived by transforming eqn. (9).

$$l = \left[\frac{6}{\pi} \frac{1}{\rho} f(t) \right]^{1/3} \quad (12)$$

$$f(t) = \frac{[C_i - C_{eq} - (C - C_{eq})]V}{N} \quad (13)$$

By inserting eqns. (7) and (10) into eqn. (13), eqn. (14) was obtained.

$$f(t) = \frac{V(C_i - C_{eq}) - V \exp[-k_1 t + \ln(C_0 - C_{eq})]}{\exp[-k_2 t + \ln N_0]} \quad (14)$$

The linear growth rate G is defined by eqn. (15).

$$G = \frac{dl}{dt} = \left(\frac{6}{\pi} \frac{1}{\rho} \right)^{1/3} \frac{1}{3} [f(t)]^{-2/3} \frac{df(t)}{dt} \quad (15)$$

$$\frac{df(t)}{dt} = \{ V(k_1 - k_2) \exp[-k_1 t + \ln(C_0 - C_{eq})] + V(C_0 - C_{eq})k_2 \} \times \exp(k_2 t - \ln N_0) \quad (16)$$

The linear growth rate of the agglomerated crystals at $t < 18$ min is plotted against $(C - C_{eq})$ in Fig. 11. The linear growth rates increased with increasing temperature, but did not depend upon $(C - C_{eq})$, as expected from

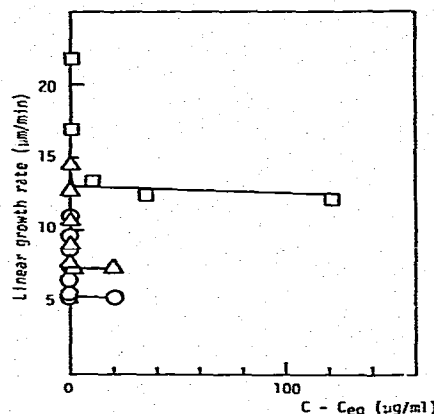


Fig. 11. Effect of temperature on the linear growth rate of agglomerates. Agglomeration temperature: \circ , 10 °C; Δ , 20 °C; \square , 30 °C.

the finding in Fig. 5. This finding indicated that agglomeration of crystals and crystallization occurred simultaneously $[(C - C_{eq}) > 0]$. In this study, it was characteristic that the linear growth rate drastically increased when $(C - C_{eq}) = 0$ at $t > 18$ min. This was sharply distinguished from a conventional crystallization without agglomeration, the kinetics of which is generally expressed by eqn. (17) [11].

$$G = K_g(C - C_{eq})^n \quad (17)$$

where K_g is the growth rate coefficient and the exponent n is the kinetic order.

The above findings indicated that the spherical crystallization process in the present study was described by three steps, i.e., initial crystal nucleation, crystallization accompanied by agglomeration at the early stage $[(C - C_{eq}) > 0, t < 18$ min] and agglomeration of crystals at the larger stage $[(C - C_{eq}) = 0, t > 18$ min]. These steps were significantly affected by the crystallization temperature as shown in Figs. 10 and 11.

REFERENCES

- 1 Y. Kawashima, M. Okumura and H. Takenaka, *Science*, **216** (1982) 1127.
- 2 Y. Kawashima, S. Y. Lin, M. Naito and H. Takenaka, *Chem. Pharm. Bull.*, **30** (1982) 1837.
- 3 Y. Kawashima, S. Aoki and H. Takenaka, *Chem. Pharm. Bull.*, **30** (1982) 1900.
- 4 H. Wadell, *J. Geol.*, **40** (1932) 443.
- 5 Y. Kawashima and C. E. Capes, *Powder Technol.*, **13** (1976) 279.
- 6 C. E. Capes and J. P. Sutherland, *Ind. Eng. Chem. Process Design Develop.*, **6** (1967) 146.
- 7 Y. Kawashima and C. E. Capes, *J. Powder Bulk Solids Technol.*, **2**(3) (1978) 53.
- 8 Y. Kawashima and C. E. Capes, *Powder Technol.*, **10** (1974) 85.
- 9 A. R. Konak, *Chem. Eng. Sci.*, **29** (1974) 1537.
- 10 P. H. Elworthy and H. E. C. Worthington, *J. Pharm. Pharmacol.*, **23 Suppl.** (1971) 101S.
- 11 J. S. Wey and R. Jagannathan, *AIChE J.*, **28** (1982) 697.